Cyclic Stiffness Photomodulation of Cell-Laden Protein-Polymer Hydrogels

Luman Liu

A thesis

submitted in partial fulfillment of the

requirements for the degree of

Master of Science in Chemical Engineering

University of Washington

2017

Committee:

Cole A. DeForest,

François Baneyx

Program Authorized to Offer Degree:

Chemical Engineering

University of Washington

Abstract

Cyclic Stiffness Photomodulation of Cell-Laden Protein-Polymer Hydrogels

Luman Liu

Chair of the Supervisory Committee:
Assistant Professor Cole A. DeForest

Although mechanical signals presented by the extracellular matrix are known to regulate many essential cell functions, the specific effects of these interactions, particularly in response to dynamic and heterogeneous cues, remain largely unknown. Here, we introduce a modular semisynthetic approach to create hydrogel biomaterials that undergo reversible stiffening in response to user-specified inputs. Employing a novel dual-chemoenzymatic modification strategy, we create fusion protein-based gel crosslinkers that exhibit stimuli-dependent intramolecular association. Linkers based on calmodulin yield calcium-sensitive materials, while those containing the photosensitive LOV2 (light, oxygen, and voltage sensing domain 2) protein give constructs whose moduli can be cycled with spatiotemporal control about living cells. We exploit these unique materials to demonstrate the significant role that cyclic mechanical loading plays on fibroblast-to-myofibroblast transdifferentiation. Our moduli-switchable materials should

prove useful for studies in mechanobiology, providing new avenues to probe and direct matrix-driven changes in cell physiology.

TABLE OF CONTENTS

LIST OF FIGURES

ACKNOWLEDGEMENTS

The author expresses sincere appreciation to his advisor Professor Cole DeForest for his guidance and encouragement, his group members Jared Shadish, Chris Arakawa, Steven Adelmund, Barry Badeau, Emily Ruskowitz, Payam Farahani, Gabrielle Benuska, Koichiro Uto and Prathamesh Gawade for their ideas and instructions on experiments, and his parents and wife Xuanyi Guo for their invaluable support.

Chapter 1. INTRODUCTION

There is a growing appreciation for the large role that mechanical signals presented by the local extracellular matrix (ECM) have on cell function. Through direct interaction with physical cues presented in the cellular ECM, these external mechanical signals are translated into internal biochemical responses that govern gene expression and cell fate decisions[1]. Seminal findings in the field of cellular mechanotransduction have demonstrated that matrix stiffness alone can drive changes in essential processes including attachment, cytoskeletal organization, migration, proliferation, and differentiation. More recently, it has been observed that cells possess mechanical "memory", storing information about past physical culture conditions to influence future behaviors[2]. These findings represent landmark observations that are rapidly changing standard practices in molecular biology and stem cell culture.

Efforts to elucidate the specific effects that ECM elasticity has on cell physiology have been performed almost exclusively using static biomaterials. While these studies have provided invaluable insight into the critical roles in which ECM stiffness regulates cellular fate, such simple systems fail to emulate biophysical dynamics known to accompany tissue/organ development, regeneration, and disease progression. Strategies to probe the biological effects of evolving tissue compliance have yielded a variety of synthetic cell culture platforms that can either soften or stiffen over time[3]. Though constructs that undergo spontaneous or cell-mediated transitions have proven beneficial in several applications, those that can be modified on demand are critical for probing biophysical responses at well-defined times. Light-mediated material alteration has proven particularly beneficial in this regard as it uniquely grants near-instantaneous and spatiotemporal

control over matrix stiffness in a potentially biocompatible manner. Material secondary photocrosslinking enables one-way stiffening[4–9], while photodegradation provides for irreversible softening[10–14], in the presence of live cells.

Beyond unidirectional elasticity changes, cells also experience cyclic loading that periodically and reversibly alter local ECM rigidity; pulsatile flow associated with the circulatory system places cyclic loads on cells virtually everywhere throughout the body, just as tissues exhibit sequential stiffening and softening during wound healing. Despite significant interest in understanding these fundamental biological processes[3,15–18], materials capable of recapitulating such dynamic and reversible stiffening remain largely undeveloped. Though a limited number of reversibly compliant biomaterials have been reported[19–27], none have proven capable of examining changes in 3D cell response to cyclic moduli alteration. Moreover, though local heterogeneities guide cell fate anisotropically within tissues, spatial control over reversible stiffening has not been previously demonstrated.

Here we introduce a generalizable strategy to create hydrogel biomaterials whose moduli can be reversibly switched in response to user-specified inputs. Wedding changes of biomolecular conformation to those in gel crosslinking density, we genetically fuse stimuli-responsive proteins with their stimuli-dependent binding partners (**Fig. 3.1a**). In the presence of the external stimulus, the responsive protein undergoes a conformational change that promotes binding to its fused partner and a shortened end-to-end length. When this stimuli is removed (or another is introduced), intramolecular protein-protein interactions are destroyed and original protein confirmation is restored. When these fusion proteins are incorporated into the hydrogel crosslinker itself,

molecular shortening translates to an elastic stiffening of the network while the extended confirmation yields a softer material (**Fig. 3.1b**). As stimuli introduction and removal can be repeated *ad infinitum*, fully reversible control over biomaterial mechanical properties is readily obtained. As several hundred proteins have been determined to undergo stimuli-dependent binding with known partners[28], many smart moduli-switchable materials responsive to distinct classes of stimuli (*e.g.*, ligands, pH, temperature, ions, light) can be readily produced.

Chapter 2. EXPERIMENTAL METHODS

2.1 PROTEIN WITH SPECIFIC N- AND C- TERMINAL AZIDO-FUNCTIONALIZATION

The gene for CaM-M13 and LOV2-Jα was obtained from addgene using polymerase chain reaction. The plasmid containing the NMT sequence was donated by Richard Kahn (Emory University). The PCR product and purified pSTEPL backbone plasmid were digested with NdeI and XhoI. The digested pSTEPL and insert sequence were ligated and transformed into chemically competent Top10 *E. coli* by heat shock. Colonies were selected and plasmids were purified. Sequencing was performed using a SimpleSeq DNA Sequencing Kit. Purified plasmid corresponding to the STEPL construct were co-transformed with plasmid containing NMT sequence into chemical competent BL21(DE3) pLysS *E. coli* (Promega) for expression.

Proteins were expressed by routine microbiology techniques. 12-azidododecanoic acid (12-ADA) was added during expression for N-terminal azido-functionalization. Bacteria cell pellets were centrifuged, resuspended and sonicated in a lysis buffer. The lysed cell mixture was centrifuged and the soluble fraction was applied to the Ni-NTA resin for 1hr. The conjugation buffer was added with an excess (20x) of desired azido-peptide to be conjugated and allowed to react at 37℃ for 4 hours. The conjugated protein was concentrated using a Amicon centrifugal spin column (10k molecular weight cut-off).

2.2 PROTEIN HYDROGEL FORMATION

Purified and lyophilized protein was redissolved in phosphate-buffered saline (PBS, pH=7.4). The thin cylindrical hydrogels were formed by SPAAC between PEG-tetraBCN (2 mM), linear PEG diazide (2 mM), and the redissolved protein (2 mM) in PBS. This gelation precursor solution was allowed to react for 2 hr between Rain-X ®-treated glass slides (500 μm spacing). For gels

formed for mammalian cell encapsulation, PEG-tetraBCN was prereacted with azido-RGDs (0.5 mM) for 1 hr prior to the addition of linear PEG diazide, crosslinker protein, and cell suspension. The gel was formed as circular droplet on a Rain-X®-treated glass slide.

2.3 PHOTOMECHANICAL TESTING

The rheological measurements of swollen hydrogels were performed on a rheometer (TA Instruments, Discovery HR-2) in between an 8-mm parallel plate geometry and a lower geometry with a built-in 470 nm blue light source (Thorlabs, M470L3-C1, 470 nm, 5 mW/cm^2). The storage modulus was measured at constant 1% strain and 1 rad/s frequency when the light source was switched by a timer cyclically at room temperature. 25 μL gel precursor was added into the 500 mm gap between the upper and lower geometry. Mineral oil was dropped around the gel precursor to maintain hydrated.

2.4 PHOTOPATTERNING CHARACTERIZATION

For reversible photobleaching and recovery recording, cylindrical LOV2 protein hydrogel was formed as aforementioned. Gels were exposed to collimated blue light (λ = 470 nm, 5 mW cm^{-2}) through a patterned photomask. The photopatterning was performed on a white light box for visualization contrast. To assess the fully reversible photo-responsive ability of the gel, blue light was turned on (30 sec) and off (60 sec) repeatedly for different patterns. Color change during the dark recovery was recorded at different time points.

2.5 CaM Hydrogel Swelling Ratio Measurement

CaM-based hydrogel volume change measurements were performed by measuring the mass change in response to different buffer conditions. Gels were washed by either Ca^{2+} buffer (1 mM $CaCl_2$, 20 mM HEPES, 50 mM NaCl) or a EGTA buffer (1 mM EGTA, 20 mM HEPES, 50 mM NaCl) for multiple cycles. For each cycle, gels were soaked in Ca^{2+} buffer for 4 hr. Gels were washed 3 times and soaked in EGTA buffer for 8 hr. Different ratio (0%, 25%, 50%, 75%) of CaM protein was used as crosslinker. Correspondingly, increased degree of volume change (0%, 4%, 8%, 12%) was observed.

2.6 PEGylated Protein SDS-PAGE Gel Shift Assay

To assess the ability for STEPL and NMT to generate homogenous protein samples with quantitative reactivity, an SDS-PAGE gel shift assay was performed on both C- and N-terminuses for 8 separately purified protein species 4 CaM (CaM-M13, CaM-M13-N_3, N_3-CaM-M13, N_3-CaM-M13-N_3) and 4 LOV2 (LOV2, LOV2-N_3, N_3-LOV2, N_3-LOV2-N_3) by SPAAC PEGylation. Each protein sample was reacted with mPEG-BCN (100x) in STEPL buffer (24 hr, 37°C). The complete disappearance of the starting protein band and the simultaneous appearance of either singly or doubly upshifted bands by the average molecular weight of a single PEG chain indicate the quantitative functionalization of purified protein from STEPL and NMT.

2.7 Circular Dichroism (CD) Spectroscopy Measurement

CD spectra were recorded on a Jasco 720 Circular Dichroism Spectrophotometer flushed with nitrogen gas. All data were corrected by blank buffer compositions. The experiments were performed in a 1mm path length quartz cuvette at a scan rate of 100nm/min. The data were collected either from a calcium buffer (1 mM $CaCl_2$, 20 mM Tris, 30 mM KCl) or a EGTA

buffer (1 mM EGTA, 20 mM Tris, 30 mM KCl). The CD spectra were measured in the far UV range from 250 to 200 nm.

2.8 3T3 Fibroblast Cell Culture

Normal and transfected NIH 3T3 fibroblast cells were culture in Dulbecco's Modified Eagle's Medium (DMEM) supplemented with fetal bovine serum (10%, Corning) and penicillin/streptomycin (1% Corning). Cells were trysinized and passaged upon reaching 90% confluency. To prepare cells for encapsulation, fibroblast cells were treated with trypsin (0.05 mM in PBS, 5min), centrifuged (1200 RPM, 4 min), and resuspended in hydrogel precursor solution (5×10^6 cells mL^{-1}). Mixtures were pipetted for a few times to ensure homogeneous encapsulation, pipetted onto coverslips, and allowed to gel (37℃, 2 hr) prior to use. After gelation, hydrogels containing encapsulated 3T3 fibroblasts were maintained using DMEM.

2.9 Cell Responses to Reversible Matrix Stiffness Modulation

NIH/3T3 fibroblasts transfected with an αSMA-luciferase and *Postn*-luciferase promoter plasmids were encapsulated (5×10^6 cells mL^{-1}) in 50% LOV2-Jα hydrogels in three polystyrene 24-well cell culture plates (Corning) under three different material conditions: 1) dark culture yielding comparatively stiff materials; 2) continuous flood exposure giving rise to softer gels; 3) shuttered light exposure (1 min on, 4 min off, $\lambda = 470$ nm, 1 mW cm^{-2}). To prepare 3T3 fibroblasts for encapsulation, hydrogel precursor solution was dropped on a circular glass coverslip in each well, allowed to gel (37℃, 2 hr) in incubator. After gelation, hydrogels containing encapsulated 3T3 fibroblasts were maintained using DMEM. Blue light was turned on in another 2 hours. The three different light conditions were maintained for 48 hours until the

hydrogels were homogenized using pestle in a cell lysis buffer. For luciferase assay, luciferase activity was measured individually and averaged from cell lysate.

Chapter 3. RESULT AND DISCUSSION

To generate stiffness-cyclable hydrogels, we perform a step-growth polymerization *via* a strain-promoted azide-alkyne cycloaddition (SPAAC) between a four-arm poly(ethylene glycol) (PEG) tetrabicyclononyne (BCN) (M_n ~ 20 kDa), a linear PEG diazide (N_3-PEG-N_3, M_n ~ 3.5 kDa), and a fusion protein end-functionalized with reactive azides (-N_3). SPAAC bioorthogonality permits responsive proteins to be introduced uniformly within idealized networks, and enables cell-laden hydrogels to be formed rapidly and robustly in serum-containing media[13,29–32]. Furthermore, precisely installed bioorthogonal handles enable almost any monomeric protein species to be used as a crosslinker without the loss-of-activity typical of site-directed mutagenesis or the uncontrollable heterogeneity that accompanies statistical reactions with endogenous amino acid residues. By varying the ratio of the azide-modified components present during gelation, the maximal extent of material response can be precisely controlled.

End-modified protein crosslinkers are prepared through an orthogonal pair of chemoenzymatic modifications (**Fig. 3.1c**). N-terminal labeling is achieved by *N*-myristoyl transferase (NMT), which promotes co-translational fatty acylation on proteins bearing the "GXXXS/T(K)" signature sequence (where X is any amino acid). NMT tolerates many synthetic analogs of its natural myristic acid substrate; enzymatic modification with 12-azidododecanoic acid (12-ADA) yields site-specific installation of azide functionality at the N-terminus[33–35]. To append bioorthogonal handles onto the C-terminus of proteins, we exploit a novel sortase-mediated transpeptidation reaction[36,37]. *Staphylococcus aureus* sortase A is a calcium-assisted transpeptidase that catalyzes the cleavage of a C-terminal sorting signal "LPXTG" with the concomitant amide linkage of a polyglycine probe and the target protein. "Sortagging" with an azide-bearing

oligoglycine permits efficient C-terminal installation of azido functionality. Here, we demonstrate that recombinant proteins bearing both enzymatic recognition sequences can be readily prepared through standard molecular cloning and expression techniques. As chemoenzymatic transformations proceed with exceptionally high labeling efficiencies[38], uniform populations of protein-based material crosslinkers can be created with any monomeric species.

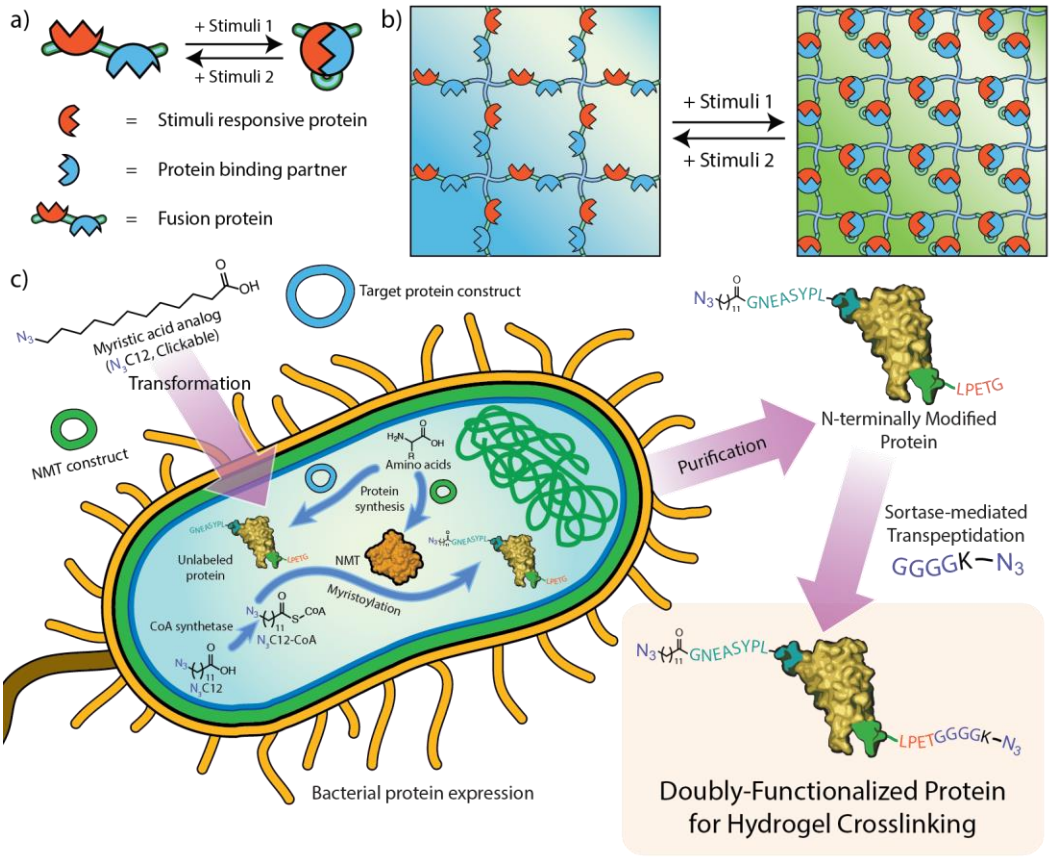

Figure 3.1. Stimuli-responsive end-functionalized protein crosslinkers.

a) Genetically encoded fusion molecules between stimuli-dependent responsive proteins with their binding partners exhibit altered confirmations and end-to-end lengths in response to external stimuli. **b)** When incorporated as a material crosslinker, intramolecular associations within the fusion protein yields reversible stimuli-dependent material stiffening. **c)** *E. coli* co-transformed with constructs for the expression of *N*-myristoyl transferase (NMT) and the target protein of interest are cultured with an azide-functionalized myristic acid analog (12-ADA). 12-ADA is

activated *in vivo* to form 12-ADA-CoA, the substrate for myristoylation of the target protein by NMT. The tagged protein is purified prior to sortase-mediated transpeptidation with an azide-functionalized polyglycine probe. The final protein is end-functionalized with reactive azides, which are exploited to form hydrogel biomaterials *via* bioorthogonal SPAAC chemistry.

Having identified a strategy to create stiffness-cyclable hydrogels using dually modified responsive proteins, we focused our initial efforts on calmodulin (CaM), a calcium-sensitive protein whose stimuli-sensitivity has been previously utilized to make dynamic materials[19,20]. Taking lead from an expansive body of genetically encoded sensors[39–41], we created a fusion of CaM and the M13 peptide fragment of myosin light chain kinase that could be dually modified for gel crosslinking. When Ca^{2+} is present, CaM undergoes a conformation changes that permits high-affinity binding with M13; when the ion is chelated away, CaM structure and intramolecular association relaxes (**Fig. 3.2a**). Following expression and modification by NMT and sortase, the end-modified N_3-CaM-M13-N_3 complex was obtained in good yield (~5 mg/L culture, non-optimized expression). Whole-protein mass spectrometry revealed exceptionally high sample purity and quantitative functionalization at both termini (**Fig. 3.2b**). Far-UV circular dichroism confirmed responsiveness of the complex to calcium (**Fig. 3.2c**), consistent with similar analysis performed on purified CaM[42]. To verify that the introduced azides were functionally accessible and maintained reactivity by SPAAC, we utilized an SDS-PAGE gel shift assay[43] involving C-/N-terminal PEGylation by BCN-monofunctionalized methoxy-PEG (mPEG-BCN, M_n ~ 10 kDa) (**Fig. 3.2b**); the complete disappearance of the starting protein band, accompanied by the simultaneous appearance of a new band upshifted by the average molecular weight of the correct number of PEG chains (0, 1, or 2, depending on condition), indicates the ability to install reactive azides site-specifically onto CaM-M13 proteins using NMT and/or sortase. Collectively, these

results demonstrate the successful generation of a bioresponsive fusion protein-based crosslinker, as well as the first utilization of two different chemoenzymatic reactions to modify a single recombinant protein.

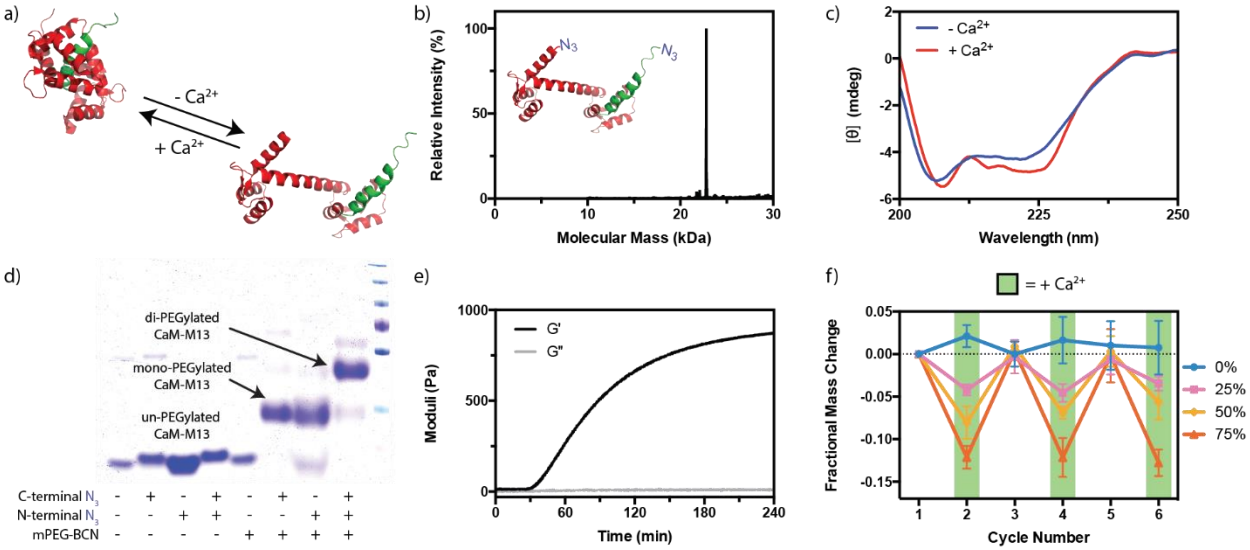

Figure 3.2. Calcium-responsive gels based on CaM-M13 intramolecular binding.

a) Calmodulin (CaM, shown in red) reversibly associates with fusion partner M13 (shown in green) in a calcium-dependent manner. **b)** Whole-protein mass spectrometry reveals that end-functionalized N_3-CaM-M13-N_3 is generated with high purity. **c)** Far-UV circular dichroism indicates that N_3-CaM-M13-N_3 undergoes stimuli-dependent conformational changes in the presence and absence of Ca^{2+}. **d)** SDS-PAGE gel shift assays with a monofunctionalized methoxy-PEG-bicyclononyne indicate that azides can be selectively and quantitatively introduced at both protein termini, and that installed azides remain active and accessible for SPAAC chemistry. **e)** Reaction of PEG-tetraBCN (2 mM), N_3-PEG-N_3 (2 mM), and N_3-CaM-M13-N_3 (2 mM), as monitored through dynamic time-sweep rheological analysis, yields robust gels on a timescale that is appropriate for cell encapsulation. **f)** CaM-M13 gels exhibit reversible swelling, as quantified by fractional mass change, in the presence and absence of Ca^{2+}. Total responsiveness scales with protein crosslinker content (0, 25, 50, 75% N_3-CaM-M13-N_3, with the balance comprised of N_3-PEG-N_3).

Calcium-responsive hydrogel networks were formed based on the SPAAC reaction of PEG-tetraBCN (2 mM), N_3-PEG-N_3 (2 mM), and N_3-CaM-M13-N_3 (2 mM). Dynamic time-sweep rheological experiments indicated gelation ~30 min after mixing, estimated by the crossover point between the elastic (G') and storage moduli (G"), and a final G' of 920 ± 50 Pa at t ~ 5 h (**Fig. 3.2e**). To assess changes in network composition in response to free-ion treatment, we examined cycled changes of mass swelling ratios in the presence or absence of Ca^{2+}. When incubated with Ca^{2+}, materials (crosslinked with 50% CaM-M13) exhibit a 5.3 ± 1.5% decrease in mass swelling ratio, reflecting the overall network constriction that accompanies CaM association with M13 (**Fig. 3.2f**). Varying the ratio of N_3-PEG-N_3 to N_3-CaM-M13-N_3 while keeping their total concentration constant (4 mM) gave materials with scaled responsiveness; gels formed with 0, 25, 50, and 75% CaM-M13 respectively exhibited 1.1 ± 2.3%, 3.0 ± 1.0%, 5.3± 1.5%, and 9.3 ± 1.7% Ca^{2+}-promoted decrease in mass swelling. In all cases, initial hydrogel mass was restored following egtazic acid (EGTA)-mediated chelation of free Ca^{2+}. Alternate treatments of Ca^{2+} and EGTA gave rise to reproducible material cyclability.

Though the CaM-M13 system proved useful in validating our overall fusion-protein-based approach, its utility in probing cell fate response to cyclic stiffening is limited: 1) Alterations to network mechanics rely on slow molecular diffusion events, preventing rapid control over material switchability. 2) Calcium signaling is involved in almost all aspects of cellular life[44], rendering it impossible to alter network parameters without also perturbing biological function. 3) Spatial control over network mechanics is not readily possible. To address each of these limitations, we identified the photoswitchable LOV2-Jα binding pair for use as a stimuli-responsive fusion

protein. Recently popularized by the optogenetics community[45–48], the light, oxygen, and voltage sensing domain 2 (LOV2) is a plant-derived photoreceptor protein with a high binding affinity towards the C-terminal Jα helix[49]. In the presence of blue light (λ = 470 nm), LOV2 initiates a photochemical reaction with a flavin mononucleotide chromophore (FMN) that results in a displacement of the Jα domain and a large conformational shift (end-to-end changes estimated to be on the order of tens of Angstroms). This change occurs rapidly in response to low levels of blue light, but reverses quickly in the dark (**Fig. 3.3a**). As cells are considered fully tolerant to light with wavelengths ≥ 365 nm[50,51], there is no concern over UV-induced DNA damage when visible light sources are employed. We anticipated that utilization of LOV2-Jα as a gel crosslinker would enable unique photoreversible and spatiotemporal control over hydrogel stiffness in the presence of live cells.

Expression of N_3-LOV2-Jα-N_3 yielded a pure species with quantitative functionalization, as confirmed by whole-protein mass spectrometry (**Fig. 3.3b**). The diazide protein exhibited the near-instantaneous shift in absorbance in response to blue light (λ = 470 nm), followed by a rapid dark recovery ($t_{1/2}$ = 12 ± 5 s, high standard deviation based on equipment sampling frequency limitations) characteristic to the unmodified LOV2[52], indicating that the protein is properly folded and that the FMN chromophore survives purification (**Fig. 3.3c**). Gel shift assays performed with mPEG-BCN confirmed that azides affixed at both the N- and C-terminus of LOV2-Jα were accessible and maintained reactivity, as well as successful generation of a light-responsive protein-based crosslinker (**Fig. 3.3d**).

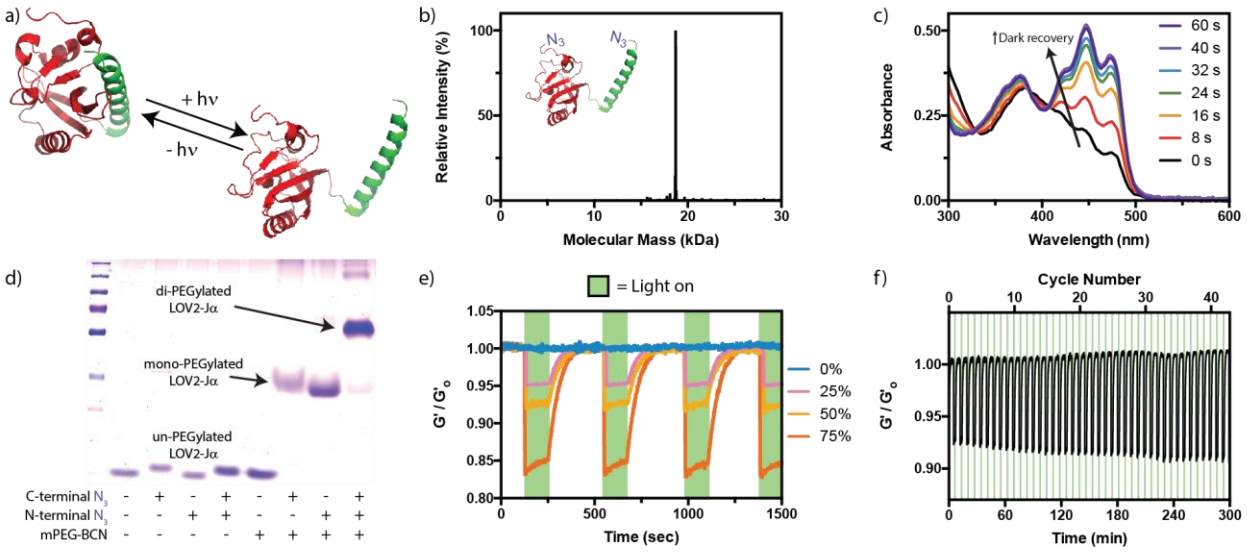

Figure 3.3. Moduli-switchable hydrogels based on LOV2-Jα intramolecular photodisassociation.

a) Light, oxygen, and voltage sensing domain 2 (LOV2, shown in red) undergoes reversible dissociation with the C-terminal Jα helix (green) in response to blue light (λ = 470 nm). This conformational change is reversed under dark conditions. **b)** End-functionalized N_3-LOV2-Jα-N_3 is obtained in high purity, as indicated by whole-protein mass spectrometry. **c)** Dark recovery photokinetic analysis of N_3-LOV2-Jα-N_3 immediately following photomediated protein disassociation. **d)** Azides can be selectively and quantitatively installed to LOV2-Jα termini, as indicated by SDS-PAGE gel shift assays with a monofunctionalized methoxy-PEG-bicyclononyne. Bioorthogonal handles remain accessible and reactive *via* SPAAC. **e)** LOV2-Jα-based gels exhibit repeated and reversible changes in elastic moduli in response to blue light (λ = 470 nm, I = 10 mW cm^{-2}), as determined by *in situ* photorheometry. Total responsiveness scales with protein crosslinker content (0, 25, 50, 75% N_3-LOV2-Jα-N_3, with the balance comprised of N_3-PEG-N_3). **f)** LOV2-Jα gel stiffness can be rapidly cycled with negligible material fatigue.

Photoswitchable gels were formed by reaction of PEG-tetraBCN (2 mM), N_3-PEG-N_3 (2), and N_3-LOV2-Jα-N_3 (2 mM). *In situ* rheometry indicated that hydrogels formed on similar timescales and with comparable mechanics as CaM-M13 materials. Photorheometry studies revealed that fully formed gels exhibited rapid softening ($t_{1/2}$ = 0.9 ± 0.2 s) in response to mild

visible light (λ = 470 nm, 10 mW cm^{-2}) (**Fig. 3.3e**). Varying the ratio of N_3-PEG-N_3 to N_3-LOV2-Jα-N_3 while keeping their total concentration constant (4 mM) gave materials with scaled responsiveness; gels formed with 0, 25, 50, and 75% LOV2-Jα respectively exhibited 0.0 ± 0.1%, 4 ± 1%, 8 ± 1%, 15 ± 1% photomediated moduli deflation. The softened state was retained until light exposure was ceased, upon which full material recovery was observed ($t_{1/2}$ = 35 ± 1 s). As expected, the timescale for gel recovery is similar but slightly slower (~3 fold) than that of LOV2's covalent separation from FMN, as some time is required for LOV2-Jα binding partners to re-associate following LOV2's conformational change. Characteristic timescales for material softening and stiffening were statistically indistinguishable for different LOV2-Jα gel compositions. By shuttering light exposure to gels, full cyclability was obtained for all materials. Negligible material fatigue was observed for 50% LOV2-Jα gels cycled >40 times over 5 hrs (**Fig. 3.3f**). Such cyclability, made possible by rapid molecular rearrangement events, has not been demonstrated previously with any other biocompatible system. Moreover, this represents the first utilization of a light-responsive protein in a materials context.

In addition to providing unprecedented temporal and cycled control over matrix properties, directed light exposure can be used to confine LOV2-Jα gel softening to user-defined physical locations (**Fig. 3.4a**). As the fast gel transition times prevent localized mechanical characterization by many conventional techniques (e.g., atomic force microscopy, nanoindentation, microrheology), we took advantage of the distinct visible color shift that accompanies LOV2 photoactivation to monitor local stiffness changes within gels (Fig. 3c); stiffer materials where LOV2 is non-covalently bound to FMN but is associated with Jα appear yellow under ambient light, while softer substrates in which LOV2 is covalently bound to FMN and disassociated from

Jα are visually clearer. Image analysis of gel color following blue light flood exposure (λ = 470 nm, 1 mW cm^{-2}, 30 s) revealed a dark recovery rate ($t_{1/2}$ = 14 ± 3 s, **Fig. 3.4b**) consistent with in-solution LOV2-Jα analysis.

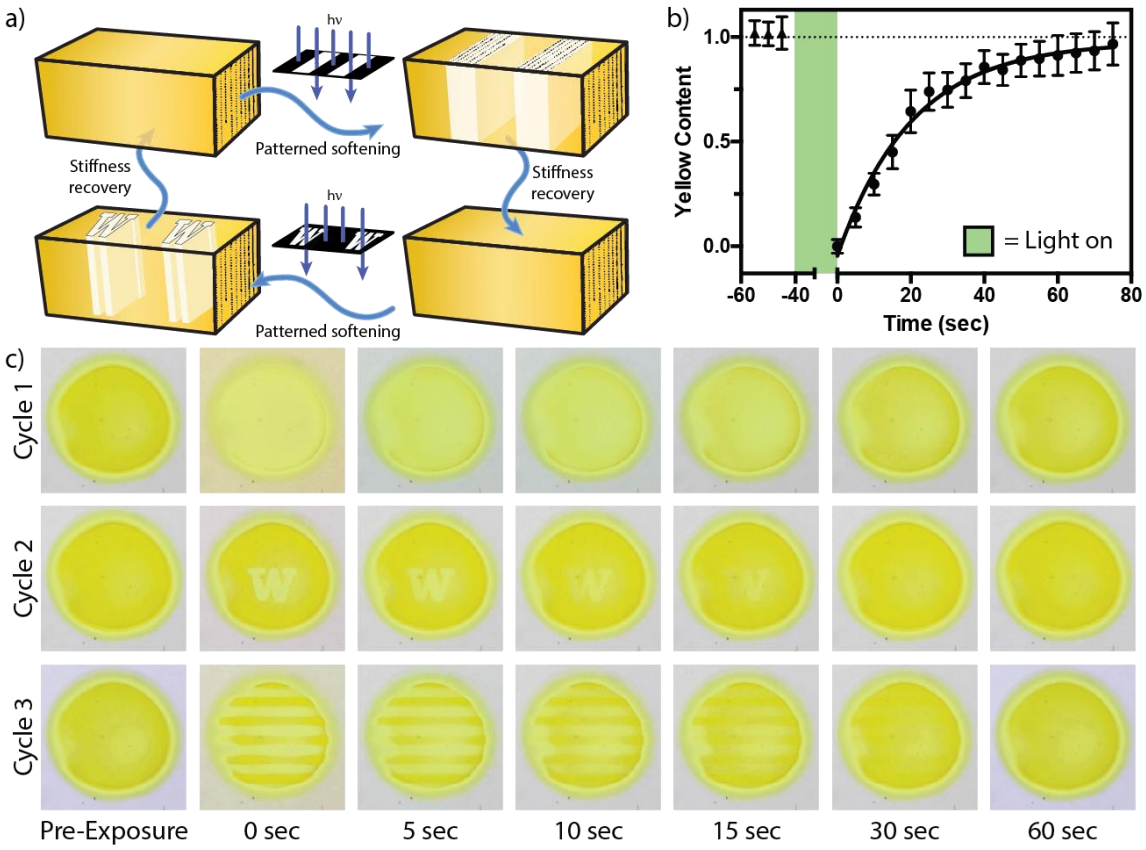

Figure 3.4. Photoreversible and spatiotemporal control over LOV2-Jα gel mechanics.

a) Stiffness-patterned hydrogels are readily generated upon masked exposure to blue light (λ = 470 nm). In the dark, these materials rapidly reset to a uniformly stiff gel. The patterning process is repeatable and scalable. **b)** LOV2-Jα gels exhibit state-dependent color profiles; stiffer gels appear yellow under ambient light, while softer substrates are visually clearer. Image analysis of hydrogel color following flood light exposure (λ = 470 nm, 1 mW cm^{-2}, 30 s) reveals fast dark recovery. **c)** Mask-based photolithography is used to confine LOV2-Jα gel softening to user-defined physical locations. Following flood light exposure and full recovery (Cycle 1), a single gel was softened in regions corresponding to the "Boundless W" logo of the University of Washington (Cycle 2). After

returning to a uniform stiffness, the gel was softened in interspaced line patterns prior to complete recovery (Cycle 3). Gel diameter ~ 1 cm, thickness ~ 200 μm.

Patterned regions of gel softening were created by traditional photolithographic techniques, whereby collimated light was shown through a photomask onto the surface of an optically thin sample. Gels were imaged before and after photopatterning; temporary changes in gel color and moduli matched masked-defined shapes (**Fig. 3.4c**). Upon complete stiffness recovery, sequential patterning was performed using the same gel and a different photomask. Results highlight the platform's unique spatiotemporal control over material compliance as well as its reversibility, where patterning can be repeated many times over to soften different material regions as desired.

Using our reversibly compliant LOV2-Jα hydrogels, we sought to examine the role of cyclic mechanical loading on myofibroblast activation in 3D. Upon injury, fibroblasts transdifferentiate into myofibroblasts that promote wound healing[53]. This activation can be regulated chemically through cytokine stimulation as well as through physical interactions with matrix substrates, and is associated with increased production of smooth muscle α-actin (αSMA) and periostin (*Postn*)[54]. Though material stiffness can drive changes in enhanced activation[55], little is known about the effects of dynamic mechanical loading on myofibroblast transformation (**Fig. 3.5a**).

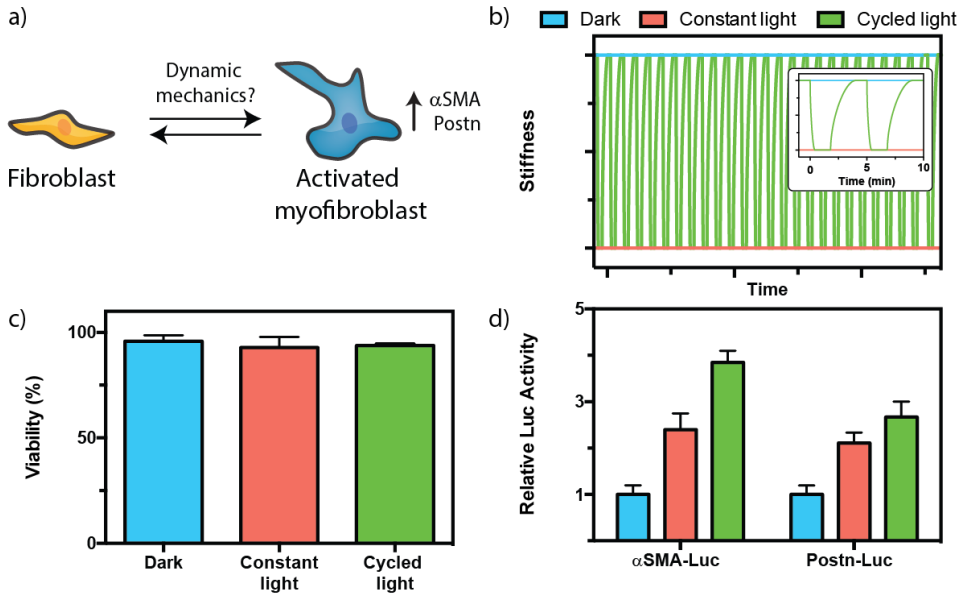

Figure 3.5. Cyclic mechanical loading drives myofibroblast activation.

a) Fibroblasts transdifferentiate into myofibroblasts in response to both chemical and physical stimulation. The role of dynamic mechanics in this process remains largely unknown. b) NIH/3T3s fibroblasts were cultured within LOV2-Jα hydrogels, each exhibiting a different time-dependent stiffness profile. Dark culture gives stiffer gels; continuous flood exposure yields comparatively soft gels; shuttered light exposure (1 min on, 4 min off) provides gels with cycled compliance. c) LIVE/DEAD staining at 48 h of cells encapsulated within this material reveals a predominantly viable population for all material treatment conditions. d) Fibroblast-to-myofibroblast transformation varies significantly with stiffness dynamics, as indicated by luciferase-based activity analysis of NIH/3T3s transfected with an αSMA-luciferase and *Postn*-luciferase promoter plasmids.

To probe these effects, NIH/3T3 fibroblasts were encapsulated (5 x 10^6 cells mL^{-1}) in 50% LOV2-Jα hydrogels and cultured for 48 hrs under three different material conditions: 1) dark culture yielding comparatively stiff materials; 2) continuous flood exposure giving rise to softer gels; 3) shuttered light exposure (1 min on, 4 min off, $\lambda = 470$ nm, 1 mW cm^{-2}) provides gels with cycled compliance (**Fig. 3.5b**). High cell viability (~95%) was observed in all conditions,

demonstrating the overall cytocompatibility of gel formation and subsequent photomechanical material alterations (**Fig. 3.5c**). To determine myofibroblast activation in each culture condition, we quantified associated changes in transcriptional programming by determining luciferase activity of cells transfected with an αSMA-luciferase promoter plasmid[56] (**Fig. 3.5d**). As expected, significant changes in αSMA promoter activity was observed for cells cultured between "stiff" and "soft" materials. Interestingly, myofibroblast activation was further enhanced within reversibly stiffening gels. This fibroblast-activating effect was further confirmed using cells transfected with a *Postn*-promoted driven luciferase reporter plasmid[56]. Observed differences in cellular transdifferentiation motivate further investigation, whereby differences in anisotropic cyclic mechanical loading is expected to play a large role in regulating powerful, yet largely unexplored, biological phenomena.

Chapter 4. CONCLUSION

The results described here illustrate a generalizable strategy to create biomaterials whose mechanics can be cycled in response to user-defined inputs. Through the first demonstrated dual-chemoenzymatic modification of a recombinant protein, we create fusion species exhibiting stimuli-dependent intramolecular association that can be used as the basis for step-growth polymerization of gels. Implementation of the technique with the photoactive LOV2 protein yielded unprecedented reversible and spatiotemporal control over network dynamics, capturing critical aspects of the cellular microenvironment. These unique materials were used to investigate biological response to cyclic loading, an important aspect of native ECM that has been difficult to replicate *in vitro*. We expect that this approach will provide a new dimension to the growing field of mechanobiology, and will provide useful in the creation of a wide variety of protein-based and stimuli-responsive materials for tissue engineering, drug delivery, and many other applications.

REFERENCES

1. Ingber, D. E. Cellular mechanotransduction: putting all the pieces together again. *Faseb J.* **20,** 811–827 (2006).
2. Yang, C., Tibbitt, M. W., Basta, L. & Anseth, K. S. Mechanical memory and dosing influence stem cell fate. *Nat. Mater.* **13,** 645–652 (2014).
3. Uto, K., Tsui, J. H., DeForest, C. A. & Kim, D.-H. Dynamically tunable cell culture platforms for tissue engineering and mechanobiology. *Prog. Polym. Sci.* (2016). doi:10.1016/j.progpolymsci.2016.09.004
4. Khetan, S., Katz, J. S. & Burdick, J. A. Sequential crosslinking to control cellular spreading in 3-dimensional hydrogels. *Soft Matter* **5,** 1601–1606 (2009).
5. Khetan, S. & Burdick, J. A. Patterning network structure to spatially control cellular remodeling and stem cell fate within 3-dimensional hydrogels. *Biomaterials* **31,** 8228–8234 (2010).
6. Khetan, S., Guvendiren, M., Legant, W. R., Cohen, D. M., Chen, C. S. & Burdick, J. A. Degradation-mediated cellular traction directs stem cell fate in covalently crosslinked three-dimensional hydrogels. *Nat Mater* **12,** 458–465 (2013).
7. Hahn, M. S., Miller, J. S. & West, J. L. Three-dimensional biochemical and biomechanical patterning of hydrogels for guiding cell behavior. *Adv. Mater.* **18,** 2679–2684 (2006).
8. Mosiewicz, K. A., Kolb, L., Van Der Vlies, A. J. & Lutolf, M. P. Microscale patterning of hydrogel stiffness through light-triggered uncaging of thiols. *Biomater Sci* **2,** 1640–1651 (2014).
9. Young, J. L. & Engler, A. J. Hydrogels with time-dependent material properties enhance cardiomyocyte differentiation in vitro. *Biomaterials* **32,** 1002–1009 (2011).
10. Raeber, G. P., Lutolf, M. P. & Hubbell, J. A. Molecularly engineered PEG hydrogels: A novel model system for proteolytically mediated cell migration. *Biophys. J.* **89,** 1374–1388 (2005).
11. Patterson, J. & Hubbell, J. A. Enhanced proteolytic degradation of molecularly engineered PEG hydrogels in response to MMP-1 and MMP-2. *Biomaterials* **31,** 7836–7845 (2010).
12. Kloxin, A. M., Kasko, A. M., Salinas, C. N. & Anseth, K. S. Photodegradable Hydrogels for Dynamic Tuning of Physical and Chemical Properties. *Science* **324,** 59–63 (2009).
13. DeForest, C. A. & Anseth, K. S. Cytocompatible click-based hydrogels with dynamically tunable properties through orthogonal photoconjugation and photocleavage reactions. *Nat. Chem.* **3,** 925–931 (2011).
14. Martens, P., Holland, T. & Anseth, K. S. Synthesis and characterization of degradable hydrogels formed from acrylate modified poly(vinyl alcohol) macromers. *Polymer (Guildf).* **43,** 6093–6100 (2002).
15. DeForest, C. A. & Anseth, K. S. Advances in Bioactive Hydrogels to Probe and Direct Cell Fate. *Annu. Rev. Chem. Biomol. Eng.* **3,** 421–444 (2012).
16. Burdick, J. A. & Murphy, W. L. Moving from static to dynamic complexity in hydrogel design. *Nat. Commun.* **3,** 1269 (2012).
17. Tibbitt, M. W. & Anseth, K. S. Dynamic Microenvironments: The Fourth Dimension. *Sci.*

Transl. Med. **4,** (2012).
18. Rosales, A. M. & Anseth, K. S. The design of reversible hydrogels to capture extracellular matrix dynamics. *Nat. Rev. Mater.* **1,** 15012 (2016).
19. Ehrick, J. D., Deo, S. K., Browning, T. W., Bachas, L. G., Madou, M. J. & Daunert, S. Genetically engineered protein in hydrogels tailors stimuli-responsive characteristics. *Nat. Mater.* **4,** 298–302 (2005).
20. Murphy, W. L., Dillmore, W. S., Modica, J. & Mrksich, M. Dynamic hydrogels: Translating a protein conformational change into macroscopic motion. *Angew. Chemie - Int. Ed.* **46,** 3066–3069 (2007).
21. Yuan, W., Yang, J., Kopečková, P. & Kopeček, J. Smart Hydrogels Containing Adenylate Kinase: Translating Substrate Recognition into Macroscopic Motion. *J. Am. Chem. Soc.* **130,** 15760–15761 (2008).
22. Gillette, B. M., Jensen, J. A., Wang, M., Tchao, J. & Sia, S. K. Dynamic Hydrogels: Switching of 3D Microenvironments Using Two-Component Naturally Derived Extracellular Matrices. *Adv. Mater.* **22,** 686–691 (2010).
23. Tamesue, S., Takashima, Y., Yamaguchi, H., Shinkai, S. & Harada, A. Photoswitchable supramolecular hydrogels formed by cyclodextrins and azobenzene polymers. *Angew. Chem. Int. Ed. Engl.* **49,** 7461–4 (2010).
24. Lin, D. C., Yurke, B. & Langrana, N. A. Inducing Reversible Stiffness Changes in DNA-crosslinked Gels. *J. Mater. Res.* **20,** 1456–1464 (2005).
25. Peng, L., You, M., Yuan, Q., Wu, C., Han, D., Chen, Y., Zhong, Z., Xue, J. & Tan, W. Macroscopic Volume Change of Dynamic Hydrogels Induced by Reversible DNA Hybridization. *J. Am. Chem. Soc.* **134,** 12302–12307 (2012).
26. Kong, N., Peng, Q. & Li, H. Rationally Designed Dynamic Protein Hydrogels with Reversibly Tunable Mechanical Properties. *Adv. Funct. Mater.* **24,** 7310–7317 (2014).
27. Rosales, A. M., Mabry, K. M., Nehls, E. M. & Anseth, K. S. Photoresponsive elastic properties of azobenzene-containing poly(ethylene-glycol)-based hydrogels. *Biomacromolecules* **16,** 798–806 (2015).
28. Berman, H. M., Westbrook, J., Feng, Z., Gilliland, G., Bhat, T. N., Weissig, H., Shindyalov, I. N. & Bourne, P. E. The Protein Data Bank. *Nucleic Acids Res.* **28,** 235–42 (2000).
29. DeForest, C. A., Polizzotti, B. D. & Anseth, K. S. Sequential click reactions for synthesizing and patterning three-dimensional cell microenvironments. *Nat. Mater.* **8,** 659–664 (2009).
30. DeForest, C. A., Sims, E. A. & Anseth, K. S. Peptide-functionalized click hydrogels with independently tunable mechanics and chemical functionality for 3D cell culture. *Chem. Mater.* **22,** 4783–4790 (2010).
31. DeForest, C. A. & Anseth, K. S. Photoreversible patterning of biomolecules within click-based hydrogels. *Angew. Chemie Int. Ed.* **51,** 1816–1819 (2012).
32. DeForest, C. A. & Tirrell, D. A. A photoreversible protein-patterning approach for guiding stem cell fate in three-dimensional gels. *Nat. Mater.* **14,** 523–531 (2015).
33. Devadas, B., Lu, T., Katoh, A., Kishore, N. S., Wade, A. C., Mehta, P. P., Rudnick, D. A., Bryant, M. L., Adams, S. P., Li, Q., Gokel, G. & Gordon, J. I. Substrate-Specificity of Saccharomyces-Cerevisiae Myristoyl-Coa-Protein N-Myristoyltransferase - Analysis of Fatty-Acid Analogs Containing Carbonyl Groups, Nitrogen Heteroatoms, and Nitrogen-Heterocycles in an Invitro Enzyme Assay and Subsequent Identific. *J. Biol. Chem.* **267,** 7224–39 (1992).
34. Heal, W. P., Wright, M. H., Thinon, E. & Tate, E. W. Multifunctional protein labeling via

enzymatic N-terminal tagging and elaboration by click chemistry. *Nat. Protoc.* **7,** 105–117 (2012).

35. Kulkarni, C., Kinzer-Ursem, T. L. & Tirrell, D. A. Selective functionalization of the protein N terminus with N-myristoyl transferase for bioconjugation in cell lysate. *ChemBioChem* **14,** 1958–1962 (2013).
36. Mao, H., Hart, S. A., Schink, A. & Pollok, B. A. Sortase-mediated protein ligation: a new method for protein engineering. *J. Am. Chem. Soc.* **126,** 2670–1 (2004).
37. Guimaraes, C. P., Witte, M. D., Theile, C. S., Bozkurt, G., Kundrat, L., Blom, A. E. M. & Ploegh, H. L. Site-specific C-terminal and internal loop labeling of proteins using sortase-mediated reactions. *Nat. Protoc.* **8,** 1787–1799 (2013).
38. Rabuka, D. Chemoenzymatic methods for site-specific protein modification. *Curr. Opin. Chem. Biol.* **14,** 790–796 (2010).
39. Nakai, J., Ohkura, M. & Imoto, K. A high signal-to-noise Ca(2+) probe composed of a single green fluorescent protein. *Nat. Biotechnol.* **19,** 137–41 (2001).
40. Tallini, Y. N., Ohkura, M., Choi, B.-R., Ji, G., Imoto, K., Doran, R., Lee, J., Plan, P., Wilson, J., Xin, H.-B., Sanbe, A., Gulick, J., Mathai, J., Robbins, J., Salama, G., Nakai, J. & Kotlikoff, M. I. Imaging cellular signals in the heart in vivo: Cardiac expression of the high-signal Ca2+ indicator GCaMP2. *Proc. Natl. Acad. Sci. U. S. A.* **103,** 4753–8 (2006).
41. Zhao, Y., Araki, S., Wu, J., Teramoto, T., Chang, Y.-F., Nakano, M., Abdelfattah, A. S., Fujiwara, M., Ishihara, T., Nagai, T. & Campbell, R. E. An expanded palette of genetically encoded Ca^{2+} indicators. *Science* **333,** 1888–91 (2011).
42. Cai, D., Ren, L., Zhao, H., Xu, C., Zhang, L., Yu, Y., Wang, H., Lan, Y., Roberts, M. F., Chuang, J. H., Naughton, M. J., Ren, Z. & Chiles, T. C. A molecular-imprint nanosensor for ultrasensitive detection of proteins. *Nat. Nanotechnol.* **5,** 597–601 (2010).
43. Carrico, I. S., Carlson, B. L. & Bertozzi, C. R. Introducing genetically encoded aldehydes into proteins. *Nat. Chem. Biol.* **3,** 321–322 (2007).
44. Clapham, D. E. Calcium Signaling. *Cell* **131,** 1047–1058 (2007).
45. Möglich, A. & Moffat, K. Engineered photoreceptors as novel optogenetic tools. *Photochem. Photobiol. Sci.* **9,** 1286 (2010).
46. Fenno, L., Yizhar, O. & Deisseroth, K. The development and application of optogenetics. *Annu. Rev. Neurosci.* **34,** 389–412 (2011).
47. Pastrana, E. Optogenetics: controlling cell function with light. *Nat. Methods* **8,** 24–25 (2011).
48. Renicke, C., Schuster, D., Usherenko, S., Essen, L.-O. & Taxis, C. A LOV2 Domain-Based Optogenetic Tool to Control Protein Degradation and Cellular Function. *Chem. Biol.* **20,** 619–626 (2013).
49. Christie, J. M. Phototropin Blue-Light Receptors. *Annu. Rev. Plant Biol.* **58,** 21–45 (2007).
50. Bryant, S. J., Nuttelman, C. R. & Anseth, K. S. Cytocompatibility of UV and visible light photoinitiating systems on cultured NIH/3T3 fibroblasts in vitro. *J. Biomater. Sci. Polym. Ed.* **11,** 439–457 (2000).
51. Wong, D. Y., Ranganath, T. & Kasko, A. M. Low-Dose, Long-Wave UV Light Does Not Affect Gene Expression of Human Mesenchymal Stem Cells. *PLoS One* **10,** e0139307 (2015).
52. Heintz, U., Schlichting, I., Afonine, P., Grosse-Kunstleve, R., Echols, N., Headd, J., Moriarty, N., Gardner, K., *et al.* Blue light-induced LOV domain dimerization enhances the affinity of Aureochrome 1a for its target DNA sequence. *Elife* **5,** e11860 (2016).

53. Hinz, B., Phan, S. H., Thannickal, V. J., Galli, A., Bochaton-Piallat, M.-L. & Gabbiani, G. The Myofibroblast. *Am. J. Pathol.* **170,** 1807–1816 (2007).
54. Kanisicak, O., Khalil, H., Ivey, M. J., Karch, J., Maliken, B. D., Correll, R. N., Brody, M. J., J Lin, S.-C., Aronow, B. J., Tallquist, M. D. & Molkentin, J. D. Genetic lineage tracing defines myofibroblast origin and function in the injured heart. *Nat. Commun.* **7,** 12260 (2016).
55. Wells, R. G. The role of matrix stiffness in regulating cell behavior. *Hepatology* **47,** 1394–1400 (2008).
56. Davis, J., Burr, A. R., Davis, G. F., Birnbaumer, L. & Molkentin, J. D. A TRPC6-Dependent Pathway for Myofibroblast Transdifferentiation and Wound Healing In Vivo. *Dev. Cell* **23,** 705–715 (2012).